International Journal of Hydrological and Environmental for Sustainability
Volume 4, Issue 2, 86-102.
e_ISSN: 2828-5050
https://www.journal.foundae.com/index.php/ijhes

Thermal Comfort and Airflow in Air-Conditioned Systems: Insights from Computational Fluid Dynamic Simulations

Jesi Pebralia*
Department of Physics,
Universitas Jambi,,
INDONESIA

Yesi Aryanti
Department of Physics,
Universitas Jambi,
INDONESIA

Lucky Zaehir Maulana
Department of Physics,
Universitas Jambi,
INDONESIA

Tika Restianingsih
Department of Materials Science and Engineering,
Institute of Science Tokyo,
JAPAN

Department of Physics,
Universitas Jambi,
INDONESIA

Marita Wulandari
Faculty of Life and Environmental Sciences,
Universitas of Tsukuba,
JAPAN

Department of Environmental Engineering,
Institut Teknologi Kalimantan,
INDONESIA

***Correspondence: E-mail:** jesipebralia@unja.ac.id

Article Info

Article history:

Received: March 10, 2025
Revised: June 15, 2025
Accepted: June 30, 2025

Abstract

Air conditioning (AC) systems are vital for ensuring thermal comfort in enclosed spaces, particularly in tropical regions like Indonesia, where high temperatures and humidity can challenge human productivity and well-being. This study investigates airflow distribution patterns in air-conditioned rooms using computational fluid dynamics (CFD) simulations, specifically employing the SST k-ω turbulence model. Simulations were conducted in a 3.5 × 3.55 × 3 m closed room with varied inlet temperatures (289.15–297.15 K) and airflow velocities (2–4 m/s). Results indicate that for every 2 K increase in inlet temperature, the average room temperature rises by approximately 1.37 K. Additionally, a 0.5 m/s increment in airflow velocity leads to an average temperature increase of 0.16 K. The airflow was observed to form a dominant jet stream from the AC inlet, flowing diagonally toward the lower part of the room, creating a low-altitude recirculation zone. This phenomenon influences thermal mixing and occupant comfort significantly. Validation of the CFD model revealed its robustness, with an average temperature deviation of 328.15 K and an Nash-Sutcliffe Efficiency (NSE) score of 0.858. Furthermore, the study suggests optimizing AC placement and operation parameters to enhance energy efficiency while maintaining comfort. These findings provide actionable insights into airflow behavior in tropical environments, promoting better design practices for cooling systems, which are crucial for sustainable development and improved living conditions in tropical climates.

Keywords: airflow; air temperature; air velocity; computational fluid dynamic;

To cite this article: Aryanti, Y., Pebralia, J., Maulana, L, Z., Restianingsih, T., and Wulandari, M. (2025). Thermal Comfort and Airflow in Air-Conditioned Systems: Insights from Computational Fluid Dynamic Simulations. *International Journal of Hydrological and Environmental for Sustainability, 4*(2), 86-102. https://doi.org/10.58524/ijhes.v4i2.768

INTRODUCTION

The data from Badan Pusat Statistics Indonesia (2023) shows a significant increase in energy consumption for air cooling system in Indonesia, reaching 31% of total household electrical energy consumption in 2022, from 24% in 2018. The use of air conditioning (AC) is currently a major requirement in the residential and commercial sectors to create thermal comfort indoors. There are various parameters that can affect thermal comfort and indirectly some of these parameters have a

relationship with indoor air quality. Therefore, there are many research studies that focus on this aspect. Among them, the influence of sound noise levels in a room (Wilani et al., 2023), as well as the parameters of temperature, humidity, and light intensity in the room (Pebralia, et al., 2024).

Air conditioners are designed to maintain temperature, humidity, and air circulation at optimal conditions, which directly affect the comfort and productivity of room occupants (Chandra et al., 2020). Thermal comfort is achieved when the temperature is in the ideal range of 295.15 to 298.15 K, where even airflow distribution is one of the important factors in achieving this condition. In this temperature range, room occupants tend to feel comfortable and are not disturbed by environmental conditions that are too hot or too cold (Juarmito et al., 2023). Uneven airflow distribution can cause problems such as overcooling and undercooling, as well as temperature diference which can cause discomfort for occupants (Ratnasari & Asharhani, 2021). In addition, unhomogeneous air distribution can lead to a poor air quality, which has a negative impact on peoples health. Research by Sahri and Hutapea (2019) shows that poor air quality in a room can reduce productivity by up to 10%.

Analysis of temperature and airflow distribution can be done through experimental methods. For example, research that has been done by direct measurements of convection heat transfer at the MLX90614 point (Putu et al., 2015), and sensor-based heat flow measurements (Pebralia et al., 2022). However, cost and time is not efficient have led many studies to turn to Computational Fluid Dynamic (CFD) methods, in order to speed up simulations and produce accurate analysis especially in a room conditions. Analysis in the CFD method is performed virtually with the help of software to produce an accurate numerical model, which can be used to test system performance. Simulation can be done at any time according to the boundary conditions (Mishbahuddin et al., 2024). CFD has proven effective in modeling airflow and heat movement in detail (Liawan et al., 2023), and is used to evaluate air distribution and thermal comfort in various settings (Seputra, 2018; Yao et al., 2022).

This purpose of this studies are to analyze the airflow distribution pattern in an air-conditioned room using CFD simulation, focusing on the effect of temperature and air velocity variations on the airflow distribution pattern. The results of this study are expected to serve as a basis for to support the design, evaluation, and analysis of air distribution in larger spaces.

METHOD

This research was conducted at the Physics Theory Laboratory, Jambi University, from December 2024 to February 2025. The equipment used in this research includes; computer, Ansys 2025 R1 software for CFD simulation, Autodesk Fusion 360 software for geometry modeling, Lutron LM-8000 formeasuring instrument to experimental data, and metric pocket for measuring room dimensions. This research uses a Computational Fluid Dyamic (CFD) numerical simulation approach with experimental data as the reference.

The research object is a closed room wich size 3.5 × 3.55 × 3 m equipped with a air conditioner unit on the wall. Measurements of room dimensions and furniture were made using a meter, while measurements of air parameters (temperature and velocity) used a Lutron LM-8000 with an accuracy of ±1.2 K for temperature and ±3% for airflow velocity. The object geometry data and measurement conditions are presented in **Table 1** and **Table 2**.

Table 1. Room geometry

Name	Size		
	Length	Widt	Height
Room	3.5 m	3.55 m	3 m
Table (a, b)	0.72 m	1.22 m	0.84 m
Cupboard a	0.4 m	0.9 m	1.80 m
Cupboard b	0.4 m	0.9 m	1.95 m
AC	0.2 m	0.8 m	0.3 m
AC Outlet	0.075 m	0.8 m	-

Table 2. Indoor air condition data at data collection points

Measurement	Measurement Point	Temperature (K)
	1	293.50
Temperature	2	297.60
289.15 K	3	294.40
Velocity 3.5 m/s	4	296.50
	5	295.50

The 3D geometry model of the room was created using Autodesk Fusion 360 software. This model was created by ignoring the small details of the furniture or room to reduce computational complexity. The 3D model of the room is shown in **Figure 1**.

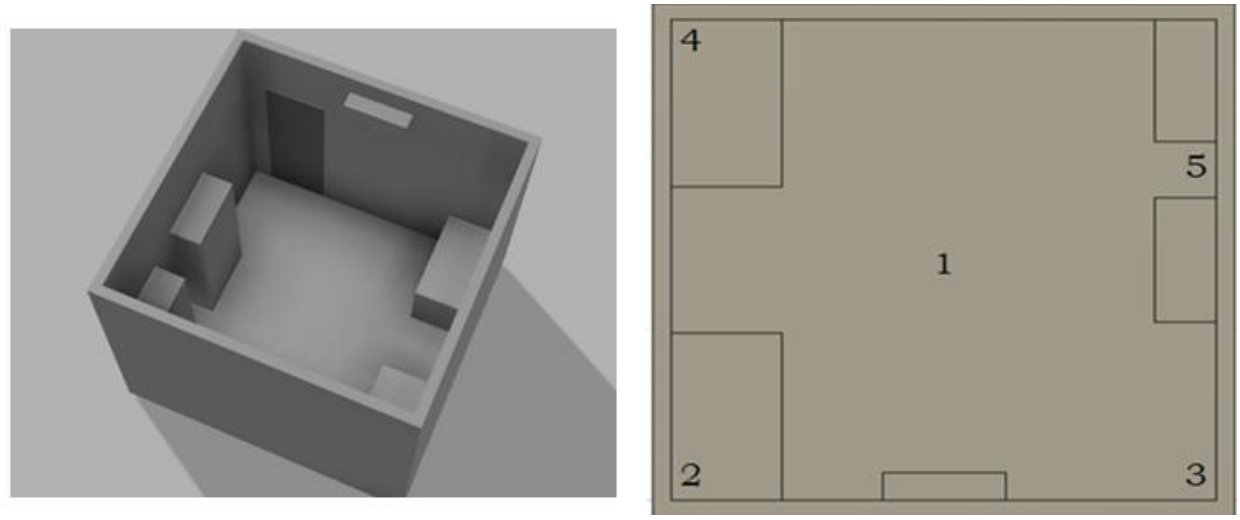

Figure 1. 3D geometry of the room in Autodesk Fusion 360

The geometry model that has been created is then imported into Ansys DesignModeler to make further arrangements before simulation. These settings include defining the fluid (air) and solid (wall, furniture) domains, determining boundary conditions, and creating a mesh. The meshing process is carried out using Ansys Meshing, with a grid size of 50 mm for the fluid domain and 5 mm for the inlet and outlet, resulting in 182 500 points and 973 411 elements.

Simulations were performed using the SST k-ω turbulence model, as it is capable of handling near-wall flows with high accuracy (Liawan et al., 2023). The transport equations for turbulent kinetic energy (k) and specific dissipation rate (ω) are formulated as follows (Anderson, 1995):

$$\frac{\partial(\rho k)}{\partial t} + \nabla \cdot (\rho k \vec{v}) = \nabla \cdot \left[\left(\frac{\mu+\mu_t}{\sigma_k}\right)\nabla k\right] + P_k - \beta\rho k\omega \quad (1)$$

$$\frac{\partial(\rho \omega)}{\partial t} + \nabla \cdot (\rho \omega \vec{v}) = \nabla \cdot \left[\left(\frac{\mu+\mu_t}{\sigma_\omega}\right)\nabla k\right] + \propto \left(\frac{\omega}{k}\right) P_k - \beta\rho\omega^2 \quad (2)$$

wich:
ρ : Fluid density (kg/m^3)
k : Turbulent kinetic energy (J/kg)
u_j : Flow velocity (m/s)
μ_t : Turbulent viscosity (kg/(m·s))
σ : Diffusion constant
S_k : Source or sink of turbulent kinetic energy (m^2/s^2)
P_k : Turbulent kinetic energy production rate (kg/m·s^3)
β : Turbulence destruction constant
ω : Specific dissipation rate (s^{-1})
$\propto$: Production constant

The wall material is assumed to be bricks with a temperature of 305.15 K, referring to the average temperature of brick walls in tropical Indonesia during the day (Santosa & Noerwasito, 2006). The air parameter values at standard conditions **(Table 3)** with density calculated using the ideal gas equation to calclulate the effect of temperature changes on density (Anderson, 1995):

$$\rho = \frac{P}{RT} \quad (3)$$

wich:
ρ : Air density (kg/m^3)
P : Air pressure (Pa)
R : Specific gas constant (R=287.05 J/(kg·K))
T : Air temperature (K)

Table 3. Air materials at standard conditions

Name	Values
Dynamic Viscosity (μ)	1.7894×10^{-5} kg/(m·s)
Heat Capacity	1006.43 J/(kg·K)
Thermal Conductivity (k)	0.0242 W/(m·K)

Air flow characteristics are analyzed using Reynolds number (Re) which is the ratio between inertial force and viscosity force. Laminar flow occurs at Re below 2000, characterized by regular flow lines. At Re values between 2000 and 4000, the flow enters a transition phase with the onset of instability. Meanwhile, turbulent flow is formed when Re exceeds 4000, which is characterized by large eddies and chaotic flow patterns (Jalaluddin et al., 2020). The Reynolds number is calculated using Equation 4 (Çengel & Cimbala, 2014):

$$Re = \frac{\rho v D}{\mu} \quad (4)$$

With:
D : Room diameter (m)
: Air flow velocity (m/s)
: Air density (kg/m^3)

To ensure the accuracy of the CFD model, validation is carried out by comparing the simulation results with experimental data. The experimental data used is temperature data measured at 5 points in the room **(Table 2)** under AC inlet conditions with a temperature of 289.15 K and a speed of 3.5 m/s. The Mean Square Error (MSE), Root Mean Squared Error (RMSE), and Nash-Sutcliffe Efficiency (NSE) methods are used to calculate the error between simulation results and experimental data (Sari & Hasanuddin, 2020).

$$MSE = \frac{1}{n}\sum_{i=1}^{n}(O_i - S)^2 \quad (5)$$

$$RMSE = \sqrt{MSE} \quad (6)$$

$$NSE = 1 - \frac{\sum_{i=1}^{n}(O_i - S_i)^2}{\sum_{i=1}^{n}(O_i - \bar{O})^2} \quad (7)$$

wich:
n : Total number of data
O_i : Observation value of i-th data
S_i : Simulated value of i-th data
$\bar{O}$: Average observation value

The visualization of the simulation results is displayed in a room cut plane designed to analyze how the air is horizontally distributed at a height of 1.5 m from the floor or in the central area of the room. The cut plane of the room can be seen in **Figure 2**.

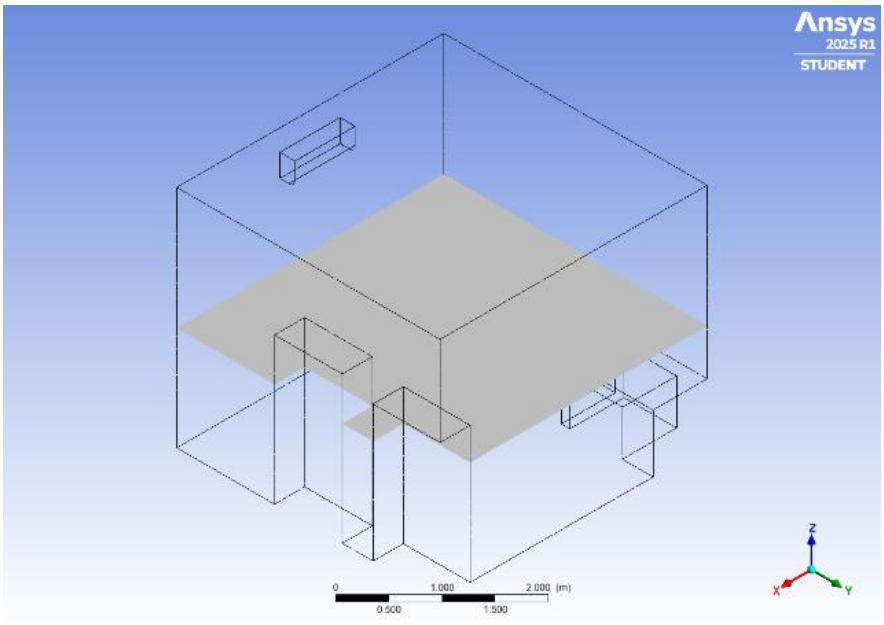

Figure 2. Horizontal plane of the center area of the object

RESULTS AND DISCUSSION

The air temperature distribution analysis in an air-conditioned room was conducted using Computational Fluid Dynamic (CFD) simulation by varying the inlet temperature and air velocity. Inlet temperature variations are; 289.15 K, 291.15 K, 293.15 K, 295.15 K, and 297.15 K constant flow velocity of 3.5 m/s. While inlet velocity variations include 2 m/s, 2.5 m/s, 3 m/s, 3.5 m/s, and 4 m/s at fixed temperature of 289.15 K. The study are includes airflow pattern, temperature distribution, velocity distribution. After the sumulation, the results will be compare to the experimental data.

The indoor airflow distribution of CFD simulation results is visualized through the airflow pattern which can be seen in **Figures 3** and **Figure 4**.

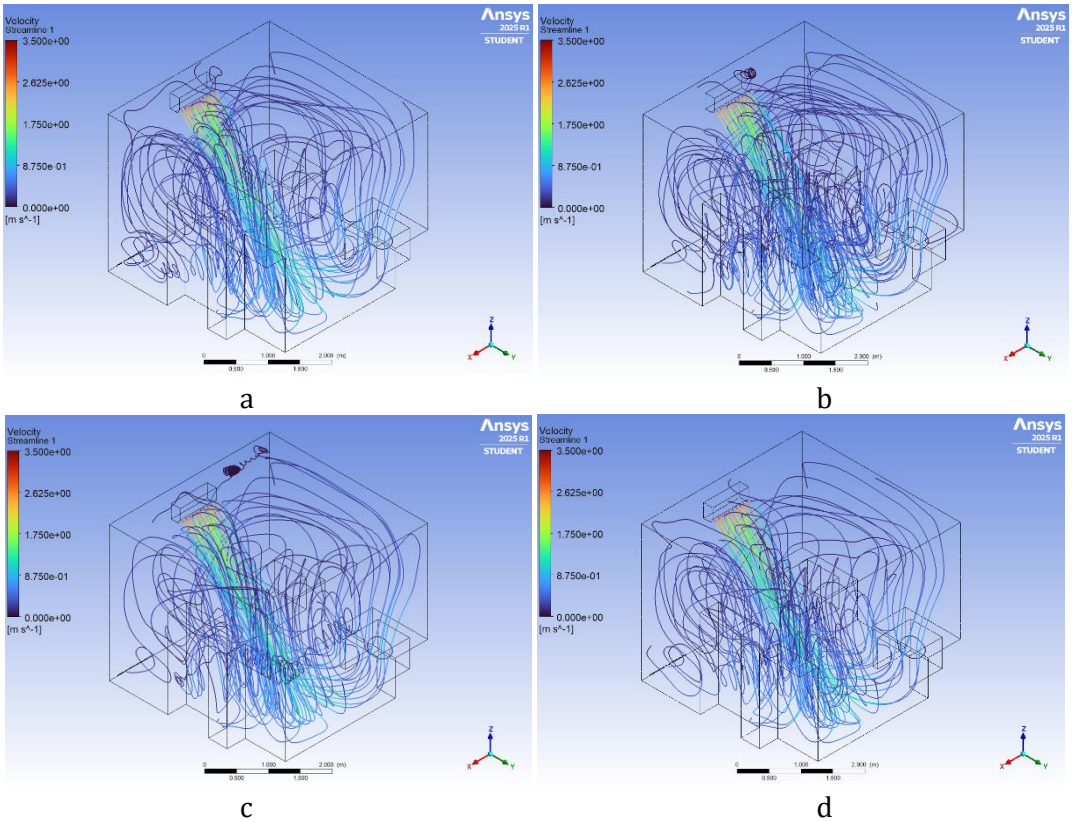

a b

c d

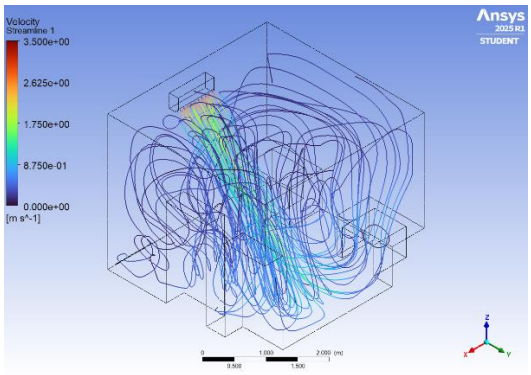

e

Figure 3. Visualization of air flow inlet temperature patterns :a. at 289.15 K, b. at 291.15 K, c. at 293.15 K, d. at 295.15 K, and e. 297.15 K)

Figure 3 presents the visualization of airflow patterns at various inlet temperatures. In general, the airflow exiting the inlet tends to move downward over the entire range of temperatures tested. At an inlet temperature of 289.15 K (a), the strong downward flow produces a circulation vortex in the lower area. As the temperature increases to 291.15 K (b), 293.15 K (c), and 295.15 K (d), downward flow remains the main characteristic, although there may be a slight decrease in flow intensity and minor changes in the size and location of the circulation vortex formed in the bottom area. Even at the highest inlet temperature of 297.15 K (e), the dominant flow is still downward, with insignificant changes to the vortices compared to lower inlet temperature conditions. Thus, based on this visualization, it can be concluded that the downward flow direction remains the main feature at all inlet temperature variations, and the changes in the shape of the vortex are relatively small.

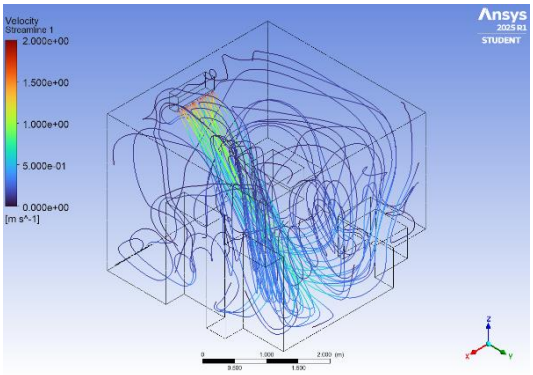

a

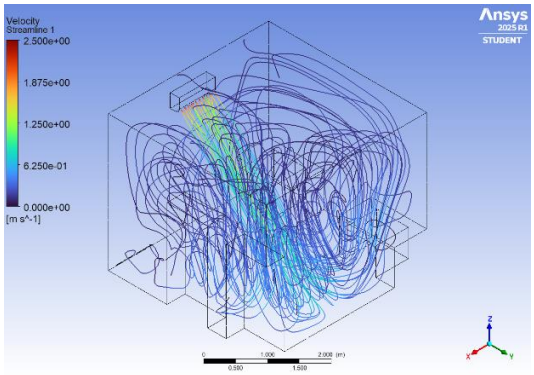

b

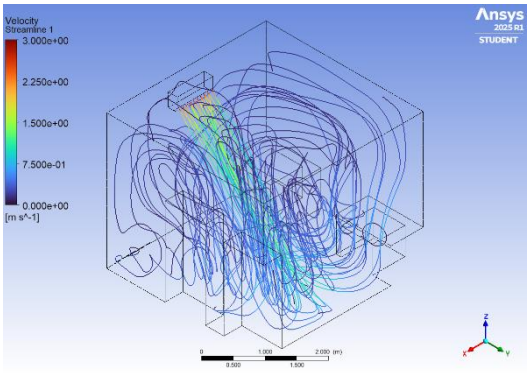

c

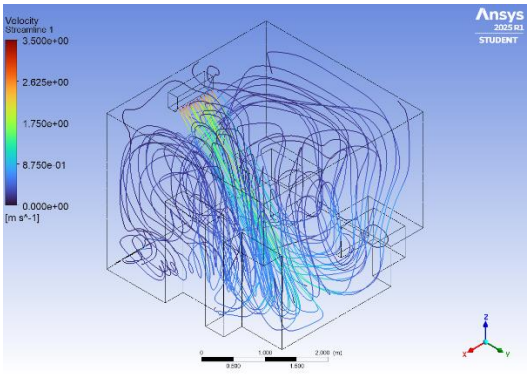

d

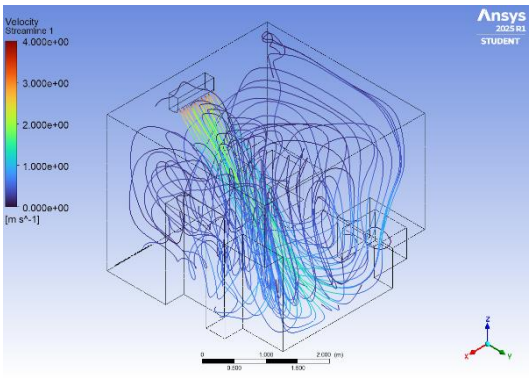

e

Figure 4. Visualization of airflow inlet velocity patterns at: a. 2 m/s, b. 2.5 m/s, c. 3 m/s, d. 3.5 m/s, and e. 4 m/s)

Figure 4 presents the visualization of airflow patterns at various inlet velocities. In general, the airflow exiting the inlet tends to move downward over the entire range of speeds tested. At an inlet velocity of 2 m/s (a), the downward flow produces a circulation pattern with a certain degree of turbulence in the lower area. As the velocity increases to 2.5 m/s (b), 3 m/s (c), and 3.5 m/s (d), downward flow remains the main characteristic, despite the increased level of turbulence in the flow pattern and circulation area at the bottom of the chamber. Even at the highest inlet velocity of 4 m/s (e), the dominant flow is still downward, but with more intense turbulence and the formation of smaller, more irregular vortices compared to the lower inlet velocity conditions. Thus, based on these visualizations, it can be concluded that the downward flow direction remains the main feature at all inlet velocity variations, and significant changes occur in the turbulence level in the lower area as the inlet velocity increases.

The indoor air temperature distribution from the CFD simulation is visualized through the temperature contours shown in **Figures 5** and **Figure 6**.

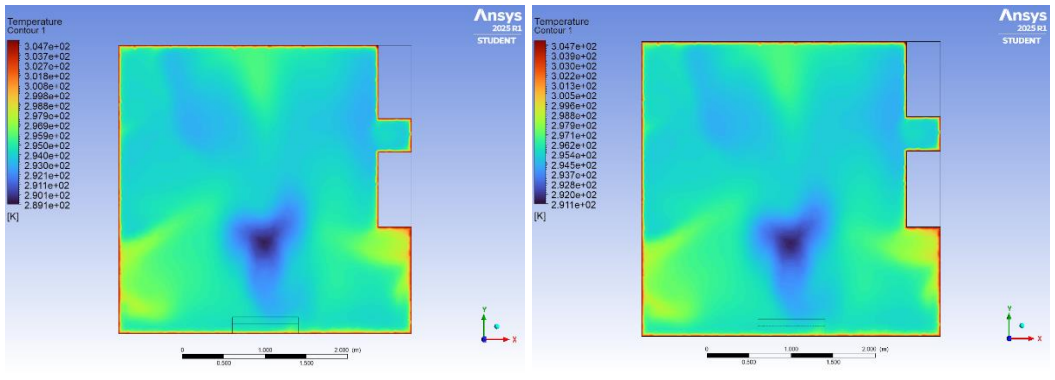

a b

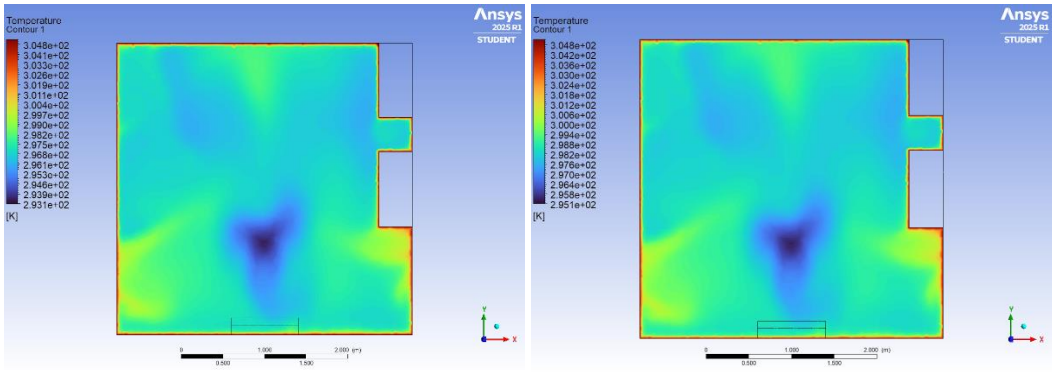

c d

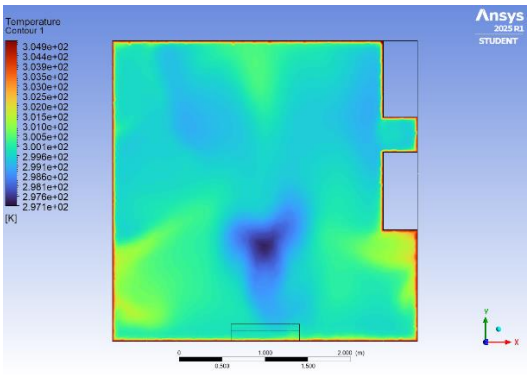

e

Figure 5. Visualization of air temperature contours at: a. 289.15 K, b. 291.15 K, c. 293.15 K, d. 295.15 K, and e. 297.15 K)

Figure 5 presents the visualization of how the temperature changes as the inlet temperature varies. At an inlet temperature of 289.15 K (a), the temperature ranges from 293.15 - 295.15 K, with higher temperatures centered around the furniture. When the inlet temperature is increased to 291.15 K (b), the temperature increases to 295.15 K, with a similar temperature distribution pattern around the furniture. At an inlet temperature of 293.15 K (c), the temperature continues to increase to 297.15 K, with higher temperature concentrated around indoor objects. The trend of increasing temperature continues at an inlet temperature of 295.15 K (d), where the temperature ranges from 297.15 – 298.15 K around the furniture. Finally, at the highest inlet temperature, 297.15 K (e), the temperature reaches 299.15 – 300.15 K, especially around the furniture. Overall, the visualization consistently shows a positive correlation between increasing inlet temperature and increasing temperature in the observed area, especially around furniture which tends to maintain higher temperatures.

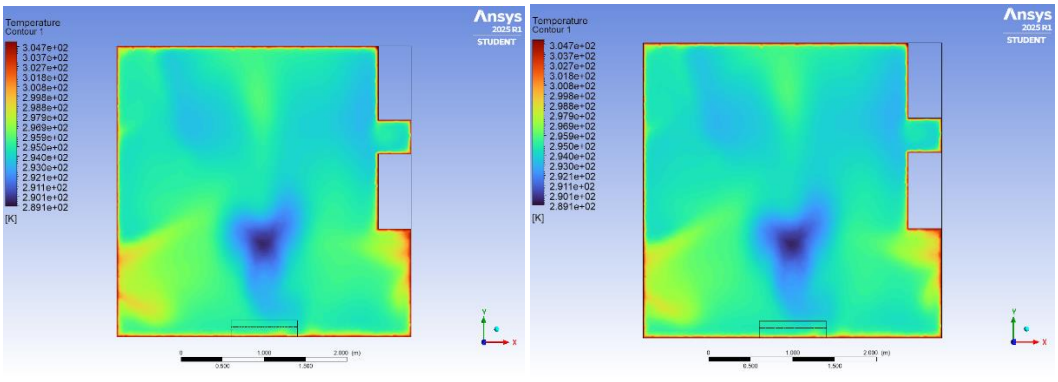

a b

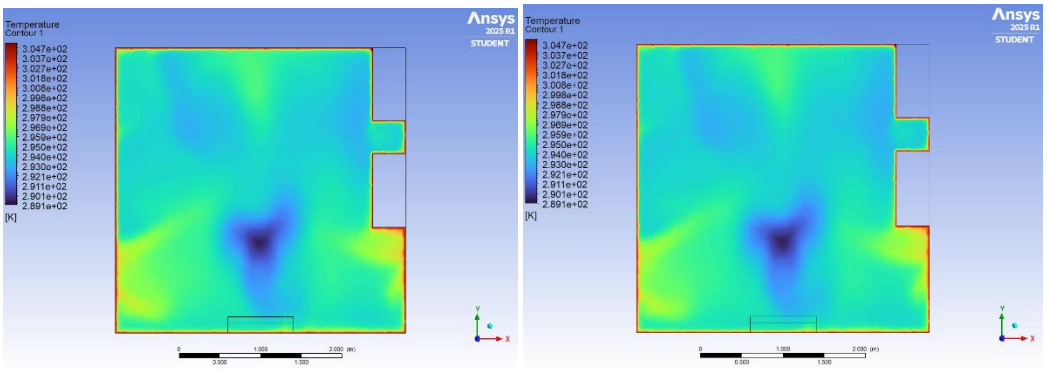

c d

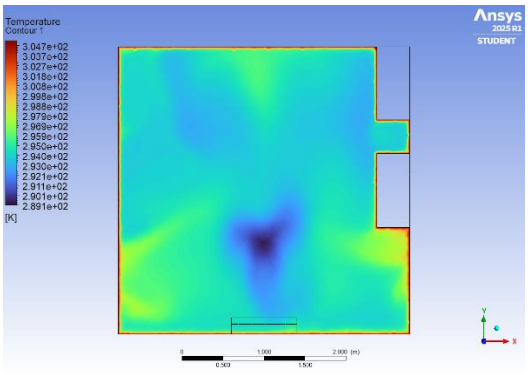

e

Figure 6. Visualization of air temperature contours at inlet velocity: a. 2 m/s, b. 2.5 m/s, c. 3 m/s, d. 3.5 m/s, and e. 4 m/s)

Figure 6 presents a visualization of how the temperature changes in the observed area as the inlet velocity varies. At an inlet velocity of 2 m/s (a), the temperature ranges from 295.15 - 297.15 K, with higher temperatures centered around the furniture. When the inlet velocity is increased to 2.5 m/s (b), the temperature remains between 295.15 - 297.15 K, with a similar temperature distribution pattern around the furniture. At an inlet velocity of 3 m/s (c), the temperature is also within the 295.15 - 297.15 K range, although the distribution appears more even. This trend continues at an inlet velocity of 3.5 m/s (d), where the temperature slightly decreases to 295.15 – 296.15 with more irregularity around the smaller furniture. Finally, at the highest inlet velocity, 4 m/s (e), the temperature shows a predominance of lower temperatures, ranging from 293.15 - 295.15 K, with minimal influence of high temperatures from the furniture. Overall, the visualizations consistently show a negative correlation between increasing inlet velocity and temperature in the observed area, especially with the reduced influence of high temperatures from furniture at higher inlet velocities.

The indoor air velocity distribution resulting from CFD simulation is visualized through velocity contours which can be seen in **Figures 7** and **Figure 8**.

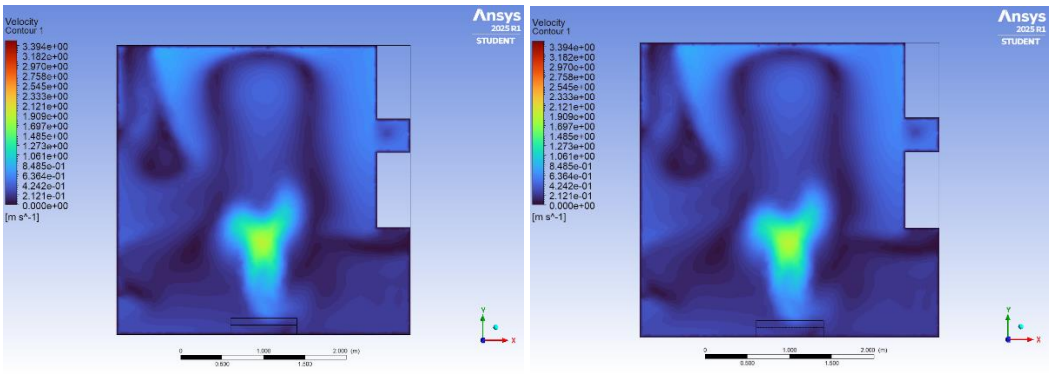

a b

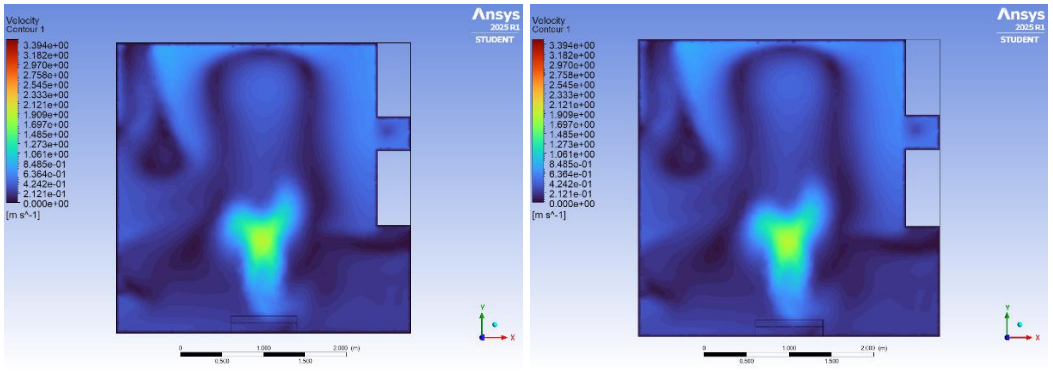

c d

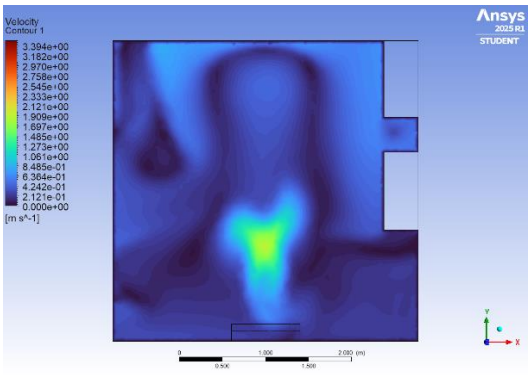

e

Figure 7. Visualization of air velocity contours for inlet temperature at: a. 289.15 K, b. 291.15 K, c. 293.15 K, d. 295.15 K, and e. 297.15 K)

Figure 7 presents a visualization of how the airflow velocity changes in the observed area as the inlet temperature varies. At an inlet temperature of 289.15 K (a), the airflow velocity ranges from 0.21 - 1.90 m/s with an upward direction in the center, and a low velocity (close to 0.00 m/s) around the furniture. When the inlet temperature is increased to 291.15 K (b), the velocity pattern and range (0.21 - 1.90 m/s with an upward direction in the center and low around the furniture) are visually similar. This condition also applies at an inlet temperature of 293.15 K (c) with an unchanged velocity range (0.21 - 1.90 m/s). Increasing the inlet temperature to 295.15 K (d) also shows a similar pattern and velocity range (0.21 - 1.90 m/s). Finally, at the highest inlet temperature of 297.15 K (e), the velocity pattern and range (0.21 - 1.90 m/s with an upward direction in the center and low around the furniture) visually show no significant changes compared to the lower inlet temperatures. Overall, the visualization shows that the variation of inlet temperature in the range of 289.15 K to 297.15 K does not result in significant changes in the airflow velocity pattern and range in the observed area.

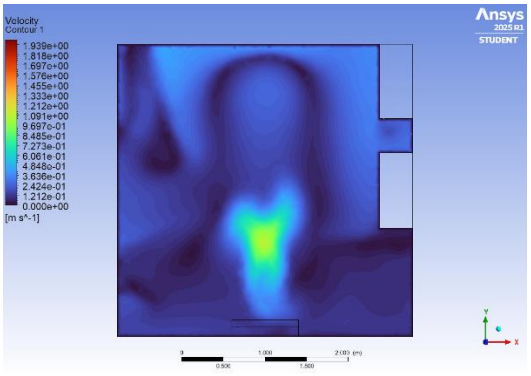

a

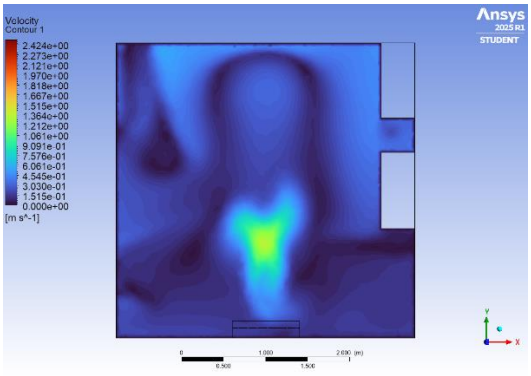

b

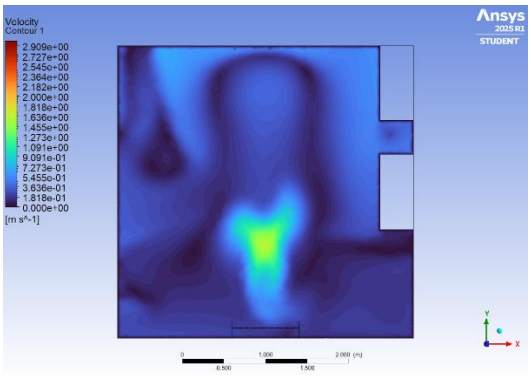

c

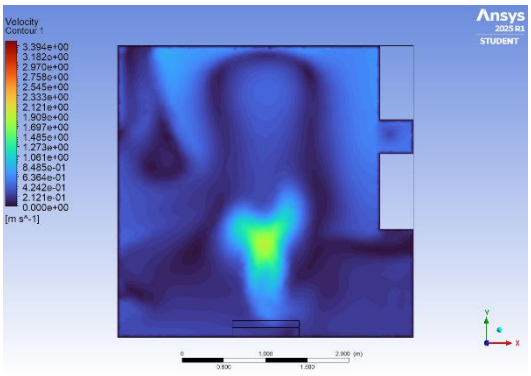

d

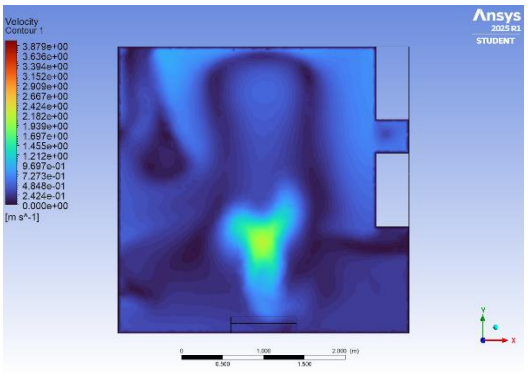

e

Figure 8. Visualization of air inlet velocity contours at: a. 2 m/s, b. 2.5 m/s, c. 3 m/s, d. 3.5 m/s, and e. 4 m/s)

Figure 8 presents a visualization of how the air flow velocity changes in the observed area as the inlet velocity varies. At an inlet velocity of 2 m/s (a), the airflow velocity ranges from 0.84 - 1.45 m/s with an upward direction in the center, and a low velocity (close to 0.00 m/s) around the furniture. When the inlet velocity is increased to 2.5 m/s (b), the velocity range in the observed area increases to 0.84 - 1.60 m/s with a similar pattern. Increasing the inlet velocity to 3 m/s (c) shows a higher velocity range of 0.10 - 1.91 m/s. At 3.5 m/s (d), the velocity range increases again to 0.11 - 2.22 m/s. Finally, at the highest inlet velocity of 4 m/s (e), the velocity range reaches 0.13 - 2.54 m/s. Overall, the visualizations consistently show a positive correlation between increasing inlet velocity and increasing airflow velocity range in the observed area. Although the flow pattern with moderate velocities in the center and low around the furniture tends to persist, the overall velocity value increases as the inlet velocity increases.

Validation of the simulation results was carried out by comparing the simulated temperature values at a variation of inlet temperature of 289.15 K and inlet velocity of 3.5 m/s at the cutting plane of the room with the temperature data from experimental measurements taken at five different points in the room. To assess the level of agreement between simulation results and experimental data, three statistical analysis methods were used, namely *Mean Squared Error (MSE)*, *Root Mean Squared Error (RMSE)*, and *Nash-Sutcliffe Efficiency (NSE)*. Low *MSE* and *RMSE* values and *NSE* values close to 1 indicate a good level of accuracy and compatibility between simulation results and experimental data (Sari & Hasanuddin, 2020).

Table 4. Air temperature values at several measurement points based on real data and simulation results

Measurement Point	Real Temperature	Simulated Temperature
1	293.5 K	293.0 K
2	297.6 K	296.9 K
3	294.4 K	294.0 K
4	296.5 K	295.9 K
5	295.5 K	295.0 K

The model validation results show an MSE value of 0.302 and RMSE of 0.55 K, which means that the difference between CFD simulation results and experimental data is very small and acceptable. The NSE value of 0.858 indicates that the model is able to explain 85.8% of the data variability, making the CFD model efficient and accurate. Thus, it can be concluded that the CFD model is well validated and reliable for predicting indoor thermal conditions.

Effect of Inlet Air Temperature Variations on Airflow Distribution Patterns

The variation of air temperature introduced through the AC unit by 289.15 K, 291.15 K, 293.15 K, 295.15 K, and 297.15 K with a fixed flow velocity (3.5 m/s) aims to analyze its impact on the flow

pattern, temperature distribution, and velocity distribution in the room. The flow characteristics at each temperature variation were analyzed using Reynolds number, as shown in **Table 5**.

Table 5. Effect of inlet temperature variation on Reynolds value

Inlet Temperature (K)	Reynolds Number
289.15	46 445.6
291.15	46 207.1
293.15	46 000.8
295.15	45 794.6
297.15	45 556.7

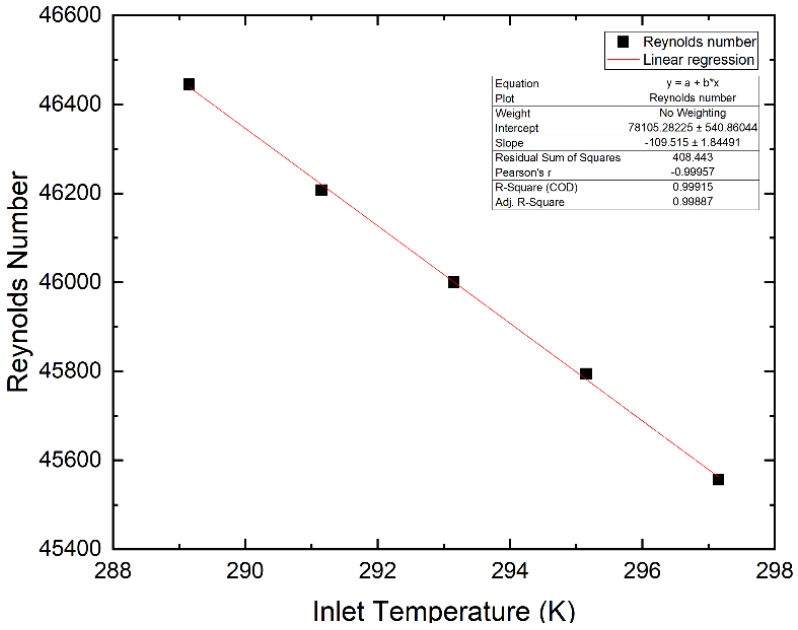

Figure 9. Graph of inlet temperature variation and Reynolds number

Figure 9 shows a graph of the linear decrease in Reynolds number (Re) as the inlet temperature increases (289.15 K to 297.15 K), from 46 445.6 to 45 556.7. The very strong relationship (R^2 = 0.99915), indicates the inlet temperature is the main determinant of the Reynolds value. The decrease in Reynolds is due to the decrease in density of the warmer air. Despite the decrease, the flow remains turbulent (Re > 4000) throughout the temperature variation.

The variation in inlet air temperature also affects the average temperature and average velocity of the indoor air. The analyzed data are presented in **Table 6**.

Table 6. The inlet temperature variation on average room temperature and air velocity

Inlet Temperature (K)	Average Temperature (K)	Average Velocity (m/s)
289.15	294.35	0.313
291.15	295.80	0.312
293.15	297.15	0.312
295.15	298.49	0.312
297.15	299.83	0.311

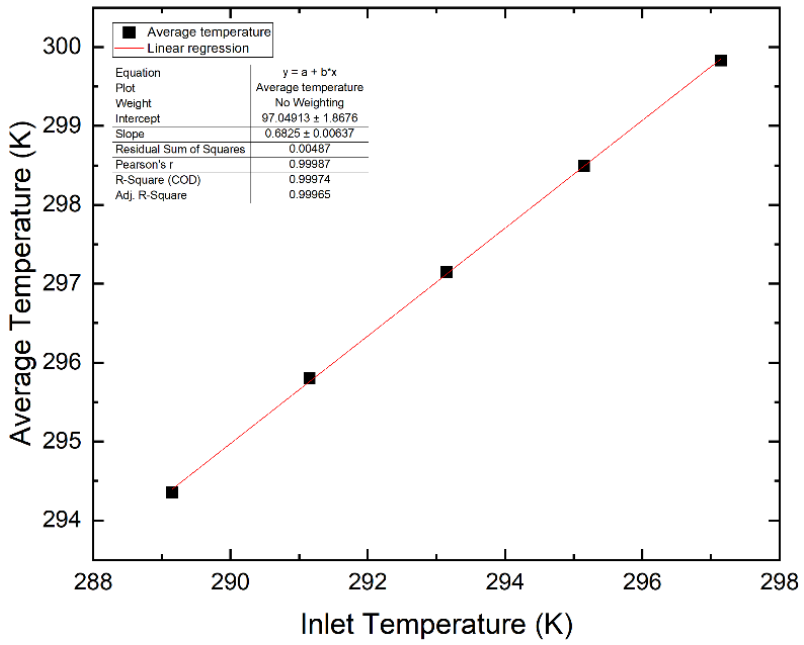

Figure 10. Graph of the effect of inlet temperature variation on room average air temperature

Figure 10 shows a graph of linear increase in room average temperature as inlet temperature increases (289.15 K - 21.293.15 K to 297.15 K – 299.83 K). The very strong relationship (R^2 = 0.99974) indicates that the inlet temperature is the main determinant of the average room temperature. Every 2 K increase in the inlet increases the room temperature by about 1.37 K.

Figure 11 shows the slight effect of inlet temperature from 289.15 K to 297.15 K on room average velocity, decreasing from 0.313 m/s to 0.311 m/s (<1% decrease). The strong relationship (R^2 = 0.8) indicates that 80% of the velocity variation can be explained by the inlet temperature. The decrease in velocity is due to lower air density at higher temperatures.

Effect of Inlet Air Velocity Variations on Air Flow Distribution Patterns

The variation of air velocity introduced through the AC unit of 2 m/s, 2.5 m/s, 3 m/s, 3.5 m/s, and 4 m/s with a fixed temperature of 289.15 K aims to analyze its impact on flow patterns, temperature distribution, and air velocity distribution in the room. The flow characteristics at each inlet velocity variation were analyzed using Reynolds number, as shown in **Table 7**.

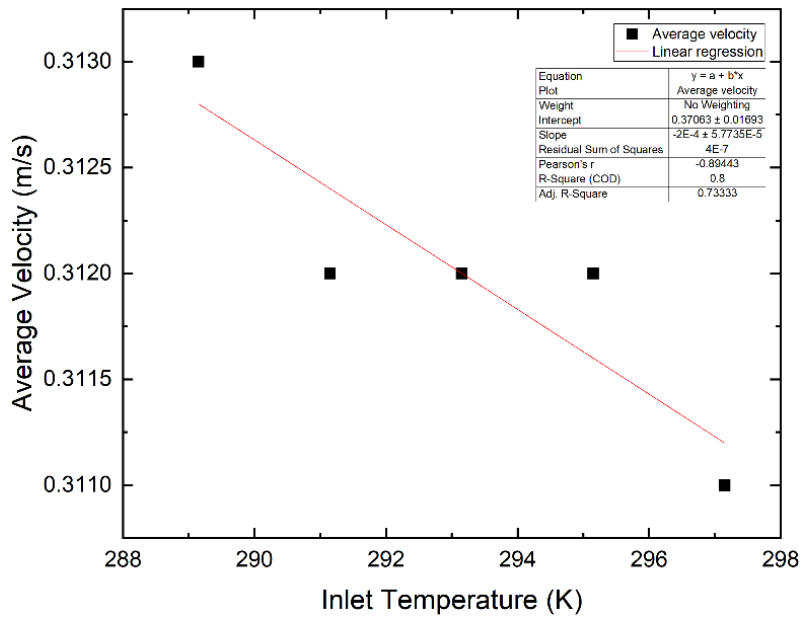

Figure 11. Graph of the effect of inlet temperature variation on room average air velocity

Table 7. Effect of inlet velocity variation on Reynolds value

Inlet Velocity (m/s)	Reynolds Number
2	25 379.5
2.5	32 636.6
3	39 893.7
3.5	46 445.6
4	53 551.0

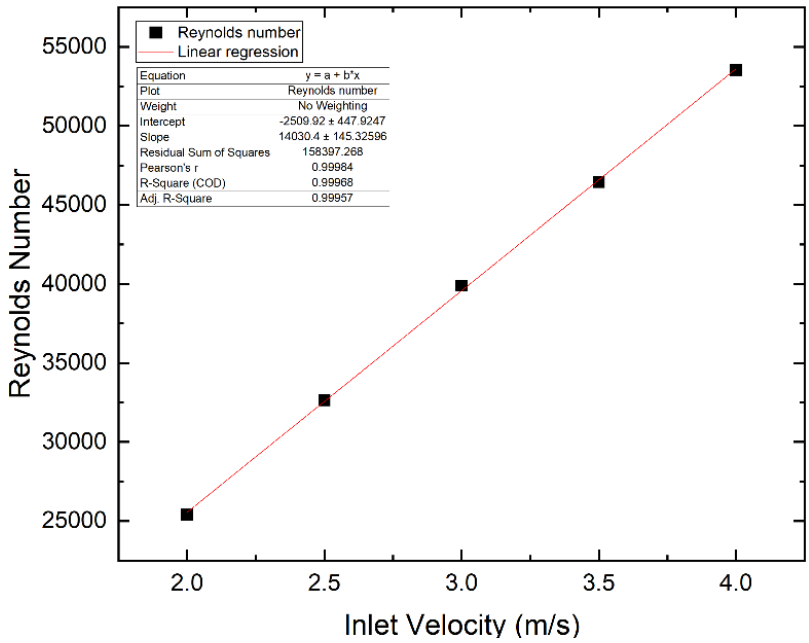

Figure 12. Graph of the effect of inlet velocity variation on Reynolds value

Figure 12 shows that the Reynolds number increases linearly as the inlet air velocity increases. The Reynolds value increases from 26 682.6 at 2 m/s to 53 365.2 at 4 m/s. This relationship has a perfect correlation with R^2 = 1.0, indicating that the inlet velocity is the main kdeterminant of the Reynolds number value. This increase indicates an increase in turbulent flow intensity.

Varying the inlet air velocity also affects the average temperature and average velocity of the indoor air. The analyzed data is presented in the following **Table 8**.

Table 8. Effect of inlet velocity variation on average room temperature and air velocity

Inlet Velocity (m/s)	Average Temperature (K)	Average Velocity (m/s)
2	294.92	0.17
2.5	294.76	0.22
3	294.61	0.27
3.5	294.35	0.31
4	294.29	0.316

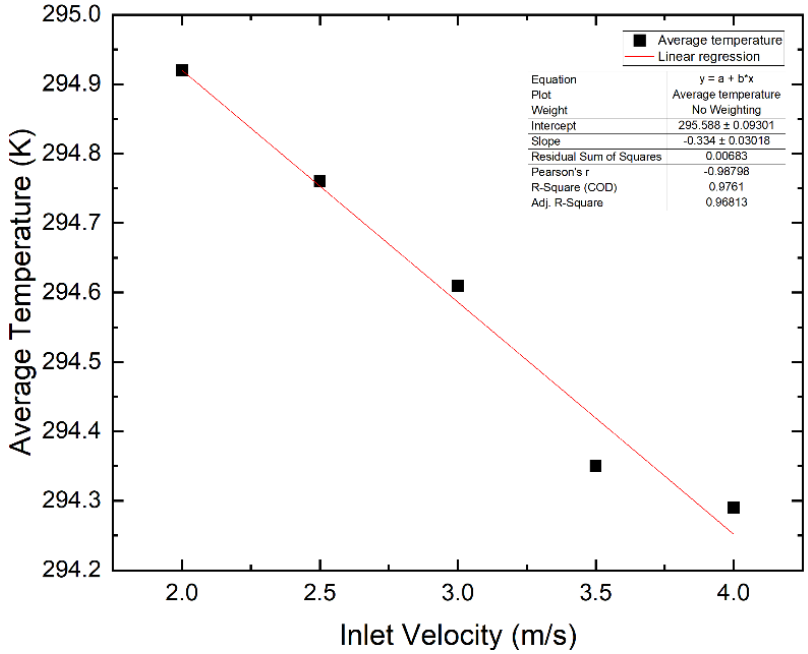

Figure 13. Graph of the effect of inlet velocity variation on room average air temperature

Figure 13 shows a linear decrease in room average temperature as inlet velocity increases (2 m/s – 297.1 K to 4 m/s – 293.95 K). The very strong relationship (R^2 = 0.99121), indicates that the inlet velocity is the main determinant of the average room temperature. Every 0.5 m/s increase in the inlet decreases the room temperature by about 0.79 K.

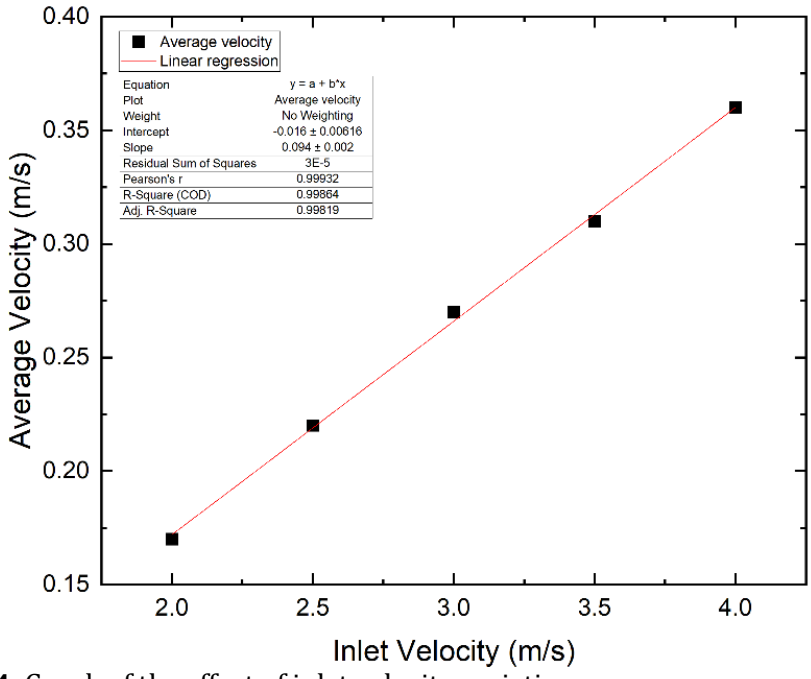

Figure 14. Graph of the effect of inlet velocity variation on room average air velocity

Figure 14 shows a graph of the increase in room average velocity as the inlet velocity increases (2 m/s to 4 m/s), from 0.214 m/s to 0.333 m/s (an increase of about 55%). The relationship is very strong (R^2 = 0.99336), indicating that 99% of the velocity variation can be explained by the inlet velocity. The increase in velocity is due to greater air momentum, thus expanding the range and intensity of air movement in the room.

CONCLUSION

Computational Fluid Dynamic (CFD) simulations successfully simulated and visualized the airflow distribution pattern in an air-conditioned room, which is dominated by turbulent flow. The high-speed airflow spreads diagonally downward, decelerates, and forms a recirculation pattern. The simulation results show good accuracy to the experimental data, with an average temperature difference of 0.55 K and the ability of the model with 85.8% of the variability of the experiment. In addition, variations in temperature and air velocity from the air conditioner have a significant effect on the flow distribution pattern. An increase in inlet temperature leads to a 1.37 K increase in average room temperature for every 2 K increase. The Reynolds number still shows turbulent flow although it only changes from 46 445.6 to 45 556.7. In contrast, increasing the inlet velocity increases the average air velocity from 0.17 m/s to 0.36 m/s, decreases the average temperature by about 0.1575 K for every increasing 0.5 m/s velocity. The significantly increases the Reynolds number from 25 379.5 to 53 551.0 which further strengthens the turbulent flow characteristics.

ACKNOWLEDGMENT

The authors would like to express their sincere gratitude to Physics Theory Laboratory, Jambi University, Indonesia for the support provided for this research. The institution's funding and continuous encouragement greatly contributed to the successful completion of this work.

CONFLICTS OF INTEREST

The authors declare no conflict of interest concerning the publication of this article. The authors also confirm that the data and the article are free of plagiarism.

REFERENCES

Çengel, Y. A., & Cimbala, J. M. (2014). Fluid mechanics: Fundamentals and applications (3rd ed.). McGraw-Hill Education.

Chandra, J. P., Putra, P., & Firdianto, A. (2020). Pola aliran udara dan distribusi temperatur diinduksi oleh sistem air conditioning. Jurnal Teknik Mesin, 9(2), 137–144.

Ichsan, D. K. (2023). Analisis pengaruh bilangan Reynold terhadap efisiensi kondensor heat exchanger menggunakan simulasi CFD. Journal of Applied Science (JAPPS), 4(2), 12–19.

Jalaluddin, J., Akmal, S., ZA, N., & Ibrahim, I. (2020). Analisa laju korosi baja karbon ST-37 dalam larutan asam sulfat dengan penambahan inhibitor ekstrak daun tembakau. Jurnal Teknologi Kimia Unimal, 8(2), 53–60.

Anderson, J. D., Jr. (1995). Computational fluid dynamics: The basics with applications. McGraw-Hill.

Juarmito, M., & Handiko, Y. D. (2023). Analisis flow simulation air conditioner duct pada konstruksi sleeper bus chassis Mercedes Benz OH 1836. Jurnal Inovasi Mesin, 5(2), 25–32.

Liawan, J. P., Tanujaya, H., & Darmawan, S. (2023). Analisis aliran udara dan kenyamanan termal di laboratorium perpindahan panas dan massa menggunakan metode Computational Fluid Dynamics (CFD). Jurnal Asiimetrik: Jurnal Ilmiah Rekayasa & Inovasi, 5(1), 123–134.

Santosa, M., & Noerwasito, V. T. (2006). Pengaruh "thermal properties" material bata merah dan batako sebagai dinding, terhadap efisiensi energi dalam ruang di Surabaya. Jurnal Teknik Arsitektur, 34(2), 147–153.

Mishbahuddin, M. H., Saputra, T. W., & Wijayanto, D. S. (2024). Pola aliran udara pada turbin angin Savonius heliks dengan variasi jumlah sudu menggunakan metode CFD. Jurnal Kinematika, 9(2), 141–152.

Pebralia, J., Amri, I., & Rifa'i, A. I. (2022). Measuring convective heat transfer in a room equipped with an air conditioner. Physics Education, 57(5), 055032.

Pebralia, J., Fendriani, Y., Afrianto, M. F., & Syaqila, C. N. (2024). Rancang bangun sistem pengukuran intensitas cahaya, suhu, dan kelembaban ruangan berbasis sensor DHT11 dan BH1750. Journal Online of Physics (JOP), 10(1), 37–42.

Putu, Y. N. N., & Pebralia, J. (2015). Studi penerapan sensor MLX90614 sebagai pengukur suhu tinggi secara non-kontak berbasis Arduino dan Labview. Prosiding Simposium Nasional Inovasi dan Pembelajaran Sains, 89–92.

Ratnasari, A., & Asharhani, I. S. (2021). Aspek kualitas udara, kenyamanan termal dan ventilasi sebagai acuan adaptasi hunian pada masa pandemi. Arsir, 24, 1–11.

Sahri, M., & Hutapea, O. (2019). Analysis and evaluation of office indoor air quality in Surabaya City. Journal of Industrial Hygiene and Occupational Health, 4(1), 1–8.

Sari, N. L., & Hasanuddin, T. (2020). Analisis performa metode moving average model untuk prediksi jumlah penderita COVID-19. Indonesian Journal of Data and Science, 1(3), 87–95.

Seputra, J. A. P. (2018). Studi distribusi udara pada ruang ber-AC untuk mencapai tingkat efisiensi energi yang optimal. ARTEKS: Jurnal Teknik Arsitektur, 3(1), 45–52.

Wilani, L., & Peslinof, M. (2023). Rancang bangun sistem monitoring kebisingan pada ruangan dengan sensor suara GY-MAX4466 berbasis Internet of Things (IoT). STRING (Satuan Tulisan Riset dan Inovasi Teknologi), 8(1), 1–8.

Yao, J., Zhong, J., & Yang, N. (2022). Indoor air quality test and air distribution CFD simulation in hospital consulting room. International Journal of Low-Carbon Technologies, 17(11), 33–37.